Inflammation, Vol. 42, No. 1, February 2019 (© 2018)
DOI: 10.1007/s10753-018-0891-7

ORIGINAL ARTICLE

TanshinoneIIA Alleviates Inflammatory Response and Directs Macrophage Polarization in Lipopolysaccharide-Stimulated RAW264.7 Cells

Shan Gao,[1] Yili Wang,[2] Dan Li,[1] Yuying Guo,[1] Meifeng Zhu,[3] Shixin Xu,[1] Jingyuan Mao,[1] and Guanwei Fan[1,4]

Abstract—TanshinoneIIA (TanIIA) has been demonstrated to possess numerous biological effects. However, the specific effect of TanIIA on macrophage polarization has not been reported. In this study, it was revealed that TanIIA might play a pivotal role in macrophage polarization. As our results indicated, cell morphology was changed in RAW264.7 cells which were treated with LPS or LPS/TanIIA (0.1 μM, 1 μM, 10 μM). Subsequently, pro-inflammatory cytokine TNF-α and anti-inflammatory cytokine IL-10 were measured by ELISA kits. Furthermore, TanIIA enhanced the expression of M2 macrophage markers (Arg1 and FIZZ1) and decreased the expression of markers associated with M1 macrophage polarization (iNOS and IL-1β). Increased expression of CD206 was also detected by flow cytometry in TanIIA-treated groups. Mechanistically, it was revealed that TanIIA modulated macrophage polarization by ameliorating mitochondrial function and regulating TLR4-HMGB1/CEBP-β pathway. In addition, increased expression of miR-155 was observed in RAW264.7 cells incubated with LPS and were effectively inhibited by TanIIA. Taken together, it was suggested that TanIIA inhibits inflammatory response and promotes macrophage polarization toward an M2 phenotype, which provides new evidence for the anti-inflammation activity of TanIIA.

KEY WORDS: TanIIA; macrophage polarization; cell elongation; mitochondrial function; TLR4-HMGB1/CEBP-β pathway.

INTRODUCTION

Long-term inflammatory response can lead to deterioration of heart failure due to continuous inflammatory signaling pathway activation [1]. In addition, due to high levels of inflammatory factors in serum, patients with rheumatoid arthritis have a much higher risk of heart failure [2]. In recent years, a large amount of clinical studies using anti-inflammatory drugs to observe the curative effect of the prevention and treatment of cardiovascular diseases, such as the clinical studies published in the NEJM, targeting inhibition of IL-1β-mediated inflammatory pathways can effectively reduce the happening of

Electronic supplementary material The online version of this article (https://doi.org/10.1007/s10753-018-0891-7) contains supplementary material, which is available to authorized users.

[1] Medical Experiment Center, First Teaching Hospital of Tianjin University of Traditional Chinese Medicine, 314 An Shan Xi Road, Nan Kai District, Tianjin, 300193, China
[2] Tianjin University of Traditional Chinese Medicine, 312 An Shan Xi Road, Nan Kai District, Tianjin, 300193, China
[3] State Key Laboratory of Medicinal Chemical Biology, Key Laboratory of Bioactive Materials of Ministry of Education, College of Life Science, Nankai University, Tianjin, China
[4] To whom correspondence should be addressed at Medical Experiment Center, First Teaching Hospital of Tianjin University of Traditional Chinese Medicine, 314 An Shan Xi Road, Nan Kai District, Tianjin, 300193, China. E-mail: fgw1005@hotmail.com

cardiovascular events [3–5]. Thus, it can be seen that the development of regulation of inflammatory response has important diagnostic and therapeutic significance in the progression of heart failure.

Macrophage is an important inflammatory regulation cell after myocardial infarction, which has the bidirectional function of pro-inflammatory and anti-inflammatory. In the early stages of inflammation (0 to 4 days), M1 (classically activated) phenotype can be detected in the heart of mice, which is mainly induced by type I inflammatory factors (such as IFN-γ, GM-CSF, and LPS). And its characteristic is high expression of iNOS; large amount of NO and ROS are synthesized in intracellular. Meanwhile, it can still secrete a large number of pro-inflammatory cytokines (IL-12, IL-23β, and TNFα, IL-1β), and chemokines (IP-10 and MIG). However, during the period of myofibroblast proliferation and reparation (10 to 14 days), there is mainly M2 (alternatively activated) phenotype [6] which is induced by IL-4, IL-13, IL-10, and M-CSF and secretes anti-inflammatory factor (IL-10 and TGF-β), chemokines (CCL24, CCL18, and CCL22), and scavenger receptor (SRs) [7]. Many studies suggest that $Ly6C^{low}$ subset plays an active role in inhibiting inflammation and promoting scar reparation during myocardial infarction. It is worth noting that M1 and M2 macrophages can undergo reversible transformation under certain conditions [8]. Therefore, how to effectively regulate the polarization of monocytes/macrophages is the key to restrain inflammatory response and promote reparation.

The mechanism of macrophage polarization is complicated and may involve several interconnected events. Previous studies have shown that bone marrow-derived macrophages (BMDMs) stimulated in culture with cytokines to induce M1 or M2 polarization displayed markedly different cell morphologies [9]. Metabolic cascades, including mitochondrial inner membrane potential and calcium loading are increasingly recognized as characteristics and controllers of macrophage activation and polarization [10, 11]. There is also a study that demonstrates that M1 activation inhibits mitochondrial function [12]. In addition to this, TLR4 is an important mediator which can regulate the polarization of macrophages by affecting the expression of HMGB1 [13] and C/EBP-β [14, 15].

TanshinoneIIA (TanIIA) is one of the main active pharmaceutical ingredients (APIs) extracted from Salvia miltiorrhiza Bge (Danshen in Chinese), which has been used clinically for the treatment of various human diseases. The pharmacological and therapeutic properties of TanIIA in the cardiovascular system have attracted interest. Emerging experimental investigations and clinical trials have demonstrated that TanIIA prevents cardiac injury, hypertrophy, and atherogenesis [16]. However, the efficacy and molecular mechanism underlying the effect of TanIIA have not been reported previously. The present study investigated whether TanIIA has an effect on macrophage polarization, and the mechanisms underlying the effects of TanIIA on macrophage polarization were evaluated *in vitro*.

MATERIALS AND METHODS

Cell Culture and Treatment

RAW264.7 murine macrophage cells were obtained from Cell Culture Center of Chinese Academy of Medical Sciences (Beijing, China). The cells were cultured in DMEM (high glucose) supplemented with 10% FBS, 100 U/mL penicillin and 100 μg/mL streptomycin at 37 °C in a humidified incubator containing 5% CO_2. For experiments, RAW264.7 cells were treated with various concentrations of TanIIA (at 0.1, 1, and 10 μM) in the presence of 1 μg/mL LPS for 6 h or 24 h. The cells treated with 0.1% DMSO were used as control.

Cell Viability and Analysis of Cell Morphology

RAW264.7 cells were seeded into a 96-well plate at a density of 2×10^4 cells/well and incubated at 37 °C in 5% CO_2 overnight. Two hundred microliters of FBS-free medium and various concentrations of TanIIA (at 0.1, 1, and 10 μM) were added to each well. After incubation for 24 h, the media in the wells were discarded and 100 μL of medium and 10 μL of MTT solution were added to each well. After incubation for 4 h, 150 μL of DMSO was added to the wells and incubated for 15 min. For cell viability determination, the absorbance values of the 96-well plate were read at 490 nm on Varioskan LUX microplate reader.

A Nikon IX73 inverted microscope was used to capture phase contrast images of cell morphology. The long axis and short axis of each cell were measured by using ImageJ software. The elongation factor was determined to be the ratio of the two axes. The area of each cell was determined by tracing cell outline.

Measuring Changes of Mitochondrial Function

The isolation of intact mitochondria from RAW264.7 cells was performed as using mitochondrial extraction kit (Solarbio, China). The cells and isolated mitochondria were seeded in a 96-well flat-bottomed plate. Mitochondrial inner membrane potential was measured by applying

the fluorescent dye JC-1 (Beyotime, China). Mitochondrial calcium loading was assessed by Fluo-4 AM (Beyotime, China).

ELISA

RAW264.7 cells were seeded in 6-well plates at a density of 5×10^5/well. After treated with various concentrations of TanIIA (at 0.1, 1, and 10 μM) in the presence of 1 μg/mL LPS for 6 h or 24 h, the supernatants were collected and the levels of TNF-α and IL-10 were determined by ELISA following the manufacturers' recommendations and quantified using Varioskan LUX microplate reader at 450 nm immediately.

RT-PCR

TRIzol reagent (Ambion) was used for RNA isolation. Then, RNA concentrations were determined by an ultramicrofluorescence spectrophotometer (DeNovix). Reverse transcription was carried out by use of HiFiScript cDNA synthesis kit (cwbiotech). Quantitative PCR (Q-PCR) assay was done using UltraSYBR mixture (cwbiotech) and analyzed using Q-PCR instrument (Lightcycler 96, Roche). Primers used in real-time PCR are shown as in Table 1. Gene expression was analyzed using the $2^{-\Delta\Delta Ct}$ method.

Flow Cytometry

RAW264.7 cells were fixed with 2% paraformaldehyde for CD206 and washed in PBS supplemented with 1% FBS and 0.01% NaN_3. Cells were incubated with CD16/32 at 4 °C for 30 min to block Fc-receptors, followed by incubation with PE-conjugated anti-mouse CD206 antibodies or isotype-matched control for 30 min on ice avoiding from light. Following thorough washing to remove excess unbound antibodies, labeled cells were analyzed by flow cytometry with FACSCalibur (BD Biosciences). Data analysis and quantification of mean fluorescence intensity were performed using FlowJo 7.6 software.

Immunofluorescence Imaging

After attaching to the cover glass, RAW264.7 cells were fixed with 4% paraformaldehyde for 15 min and then blocked with 5% goat serum in 1× PBS at RT for 30 min. Primary antibodies diluted 1:100 in PBS were applied to the cells at 4 °C overnight. The cells were then incubated with secondary antibodies diluted 1:200 in PBS at RT for 1 h and counterstained with DAPI and washed before imaging using a Leica DM6000B upright fluorescent microscope. Cell fluorescence was quantified using ImageJ software.

Western Blot Analysis

Protein samples were obtained from the lysates of cultured cells and the protein concentration was determined using the bicinchoninic acid (BCA) protein detection system Proteins were then denatured in a 5× loading buffer at 100 °C for 5 min and separated by 12% SDS-PAGE. Proteins were transferred from the gels onto a PVDF membrane and blocked with Quickblock blocking buffer (TBSTw) for 2 h. The membranes were then incubated with appropriate primary antibodies overnight at 4 °C. After washed with TBST three times, membranes were incubated with secondary antibodies for 2 h at room temperature. The protein samples were visualized using ECL western blotting substrate and imaged immediately using C-DiGit 3600 (Li-Cor, USA).

Statistical Analysis

All of the experiments were repeated at least three times. Results were shown as the mean ± standard deviation (SD). The statistical significance was determined using a two-tailed Student's t test and a p value < 0.05 was considered to be statistically significant. All of the calculations were performed using GraphPad Software.

Table 1. List of Primer Pairs Used for qRT-PCR

Primer	Forward (5′-3′)	Reverse (5′-3′)
iNOS	CCTGTGTTCCACCAGGAGAT	CCTGTGTTCCACCAGGAGAT
IL-1β	CCTGTGTTCCACCAGGAGAT	CCTGTGTTCCACCAGGAGAT
Arg1	CCTGTGTTCCACCAGGAGAT	CCTGTGTTCCACCAGGAGAT
FIZZ1	TGCTGGGATGACTGCTACTG	TGCTGGGATGACTGCTACTG
GAPDH	AACTTTGGCATTGTGGAAGG	ACACATTGGGGGTAGGAACA

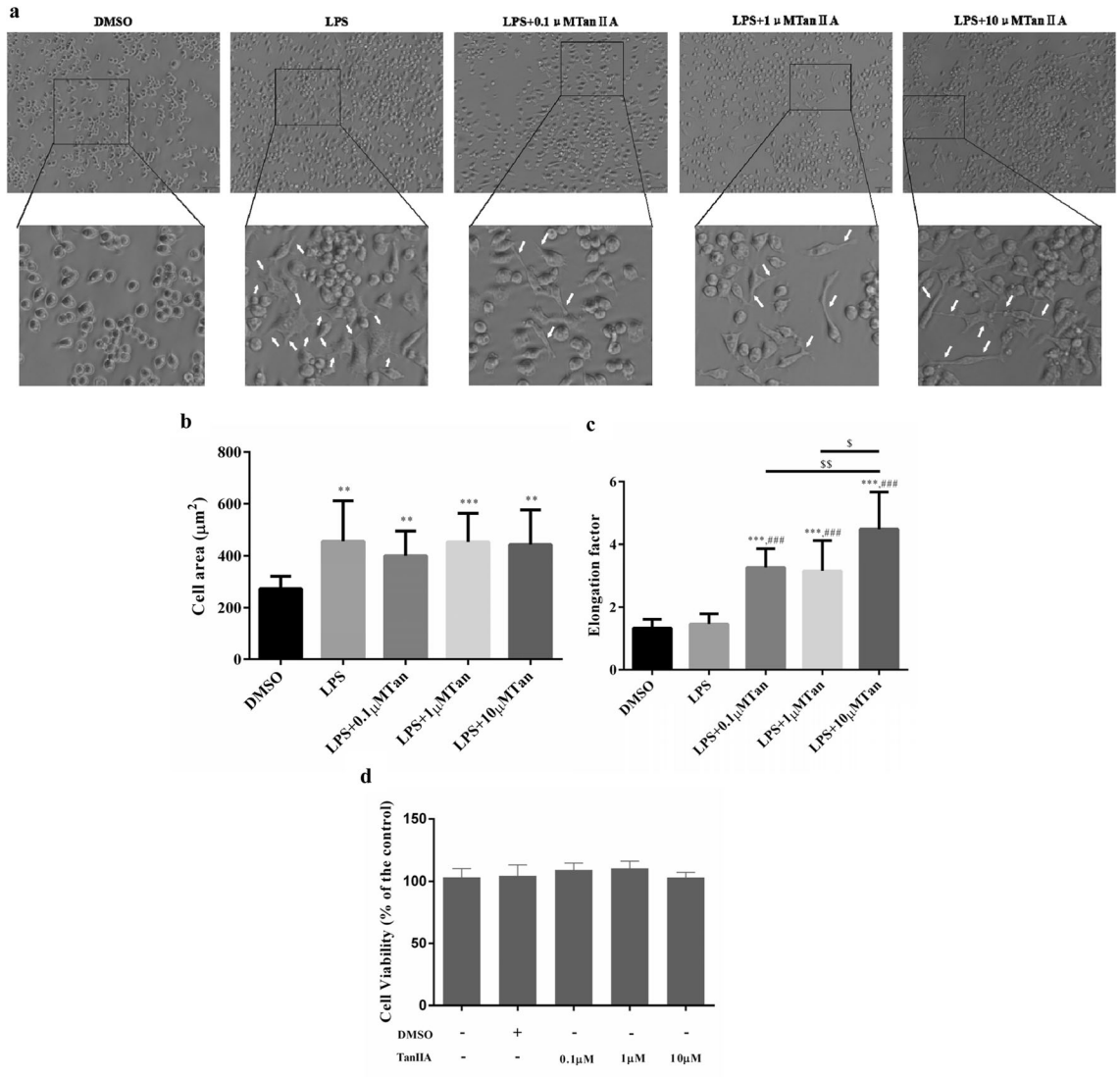

Fig. 1. The effect on RAW264.7 cell morphology and viability of TanIIA treatment. **a** Phase contrast images of RAW264.7 cells untreated or treated with LPS or LPS/TanIIA (0.1 μM, 1 μM, 10 μM) (scale bar 50 μm). **b** Quantification of area for each group. **c** Quantification of elongation factor for each group. **d** Cell viability of RAW264.7 cells was measured by MTT. Error bars indicated mean ± SD for three separate experiments. $^{**}p < 0.01$, $^{***}p < 0.001$ compared with the control group; $^{\#\#\#}p < 0.001$ compared with the LPS group; $^{\$}p < 0.05$; $^{\$\$}p < 0.01$.

RESULTS

The Effect on RAW264.7 Cells Morphology and Viability of TanIIA Treatment

The morphology of RAW264.7 cells was mainly rounded shape. As shown in Fig. 1a, b, after stimulated with LPS, the cells displayed markedly different morphologies and larger cell area compared with control group. Simultaneously, Fig. 1a, c showed us that the cells stimulated in culture with TanIIA exhibited more elongated morphologies. As had been reported by other groups [9], M2 macrophages showed an elongated cell shape compared with M1. To assess cytotoxicity of TanIIA on RAW264.7 cells, MTT assay was used. As shown in Fig. 1d, the viability of the cells was not significantly affected by TanIIA at different concentrations (0 μM, 0.1 μM, 1 μM, 10 μM) for 24 h.

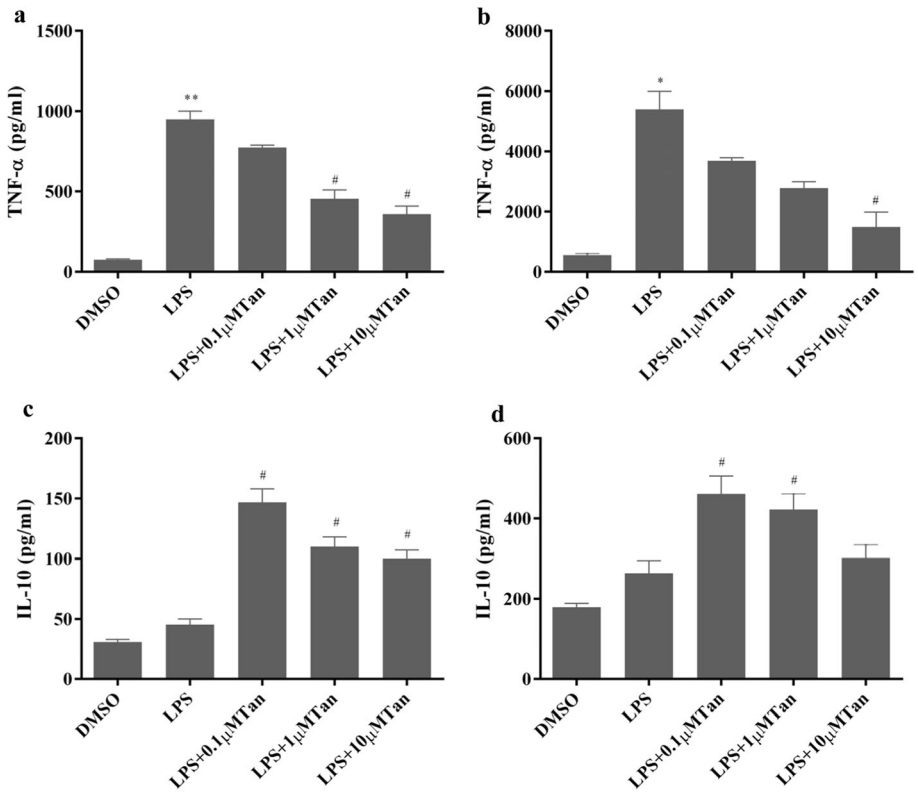

Fig. 2. Pro- and anti-inflammation of TanIIA in LPS-stimulated RAW264.7 cells. **a**, **b** The concentration of TNF-α from LPS treated or LPS/TanIIA treated for 6 h or 24 h. **c**, **d** The concentration of IL-10 from LPS treated or LPS/TanIIA treated for 6 h or 24 h. Error bars indicated mean ± SD for three separate experiments. $*p < 0.05$, $**p < 0.01$ compared with the control group; $^{\#}p < 0.05$ compared with the LPS group.

Pro- and Anti-inflammation of TanIIA in LPS-Stimulated RAW264.7 Cells

To further estimate the pro- and anti-inflammation of TanIIA, we detected the concentration of TNF-α (pro-inflammatory factor) and IL-10 (anti-inflammatory factor) [17] in the supernatants. As shown in Fig. 2a, b, TanIIA effectively inhibited TNF-α secretion by LPS. It is noteworthy that the concentration of IL-10 increased following treatment of TanIIA at different concentrations for 6 h or 24 h (Fig. 2c, d).

TanIIA Upregulates Expression of Markers for M2 Macrophage and Promotes M2 Polarization in LPS-Stimulated RAW264.7 Cells

To explore whether TanIIA could regulate the polarization of LPS-stimulated RAW264.7 cells, real-time PCR assay was used to assess mRNA expressions of macrophages with different phenotypes. In the present study, the level of M1 phenotype markers iNOS and IL-1β increased significantly in LPS-stimulated RAW264.7 cells, whereas they were inhibited by TanIIA treatment for both 6 h and 24 h (Fig.S1a and Fig. 3a). As shown in Fig. S1b, the mRNA of M2 phenotype markers Arg1 and FIZZ1 expressed low level by TanIIA treatment for 6 h. By contrast, they increased significantly by TanIIA treatment for 24 h compared with control and LPS group (Fig. 3b). As shown in Fig. 3c–e, the results of western blot analysis for the protein expression of different phenotypes were similar to those obtained by real-time PCR.

CD206, the macrophage mannose receptor [18], was also the marker of M2 phenotype. From the results of flow cytometry, we found that there was no difference of CD206 between each group by LPS and TanIIA treatment for 6 h (Fig. S2), whereas a significant upregulation of CD206 was detected in TanIIA groups for 24 h compared with the other two groups (Fig. 4a).

We also used immunofluorescence imaging to assess the polarization of LPS-stimulated RAW264.7 cells which were treated by TanIIA simultaneously. As shown in Fig. 4b, c, LPS-stimulated RAW264.7 cells displayed a larger and more irregular morphology (which were called

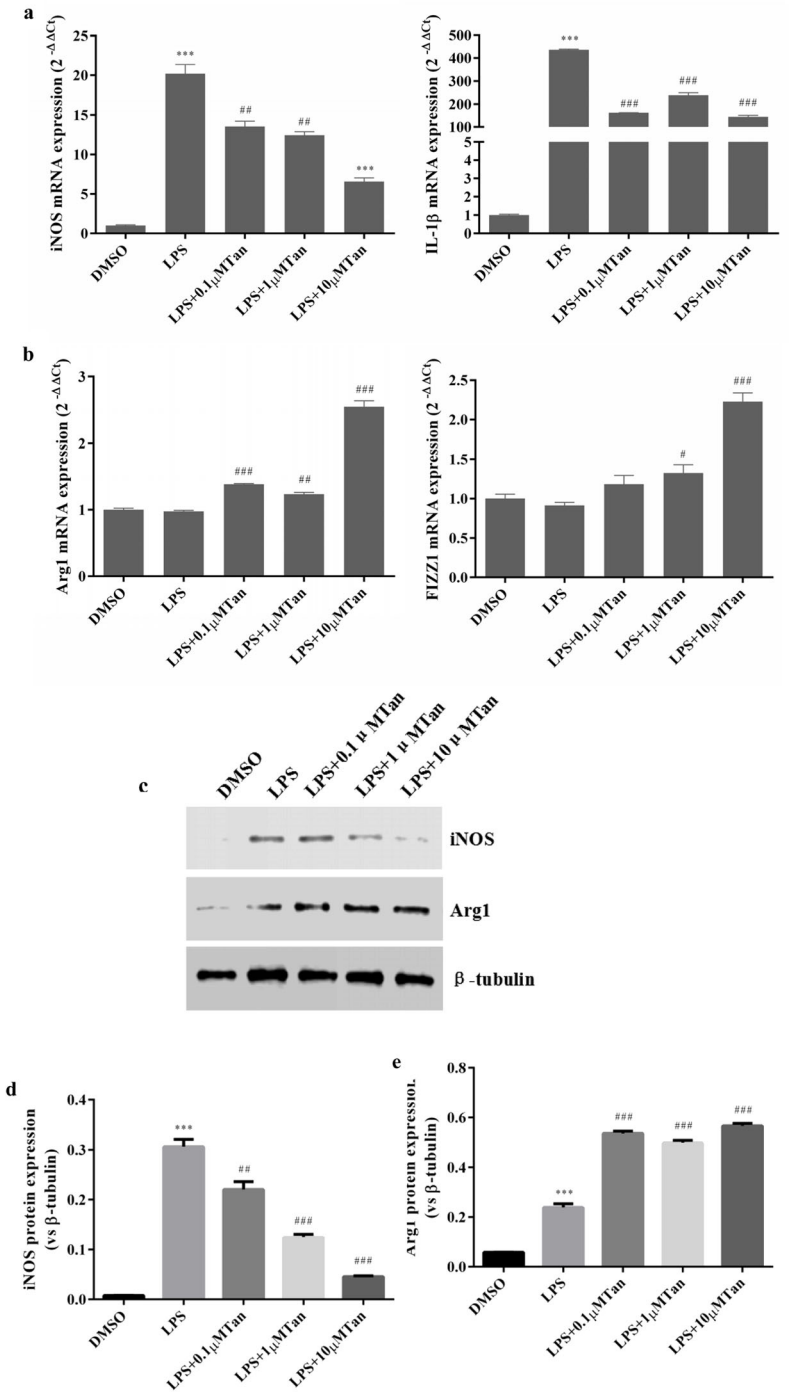

Fig. 3. TanIIA regulated expression of markers for M1 and M2 macrophage. **a** The expression of M1 macrophage phenotype-related genes from LPS treated or LPS/TanIIA treated for 24 h. **b** The expression of M2 macrophage phenotype-related genes from LPS treated or LPS/TanIIA treated for 24 h. **c**–**e** Representative Western blot of iNOS, Arg1, and β-tubulin from LPS treated or LPS/TanIIA treated for 24 h and quantitative data of average across three separate experiments. Error bars indicated mean ± SD for three separate experiments. $^{***}p < 0.001$ compared with the control group; $^{###}p < 0.001$, $^{##}p < 0.01$, $^{#}p < 0.05$ compared with the LPS group.

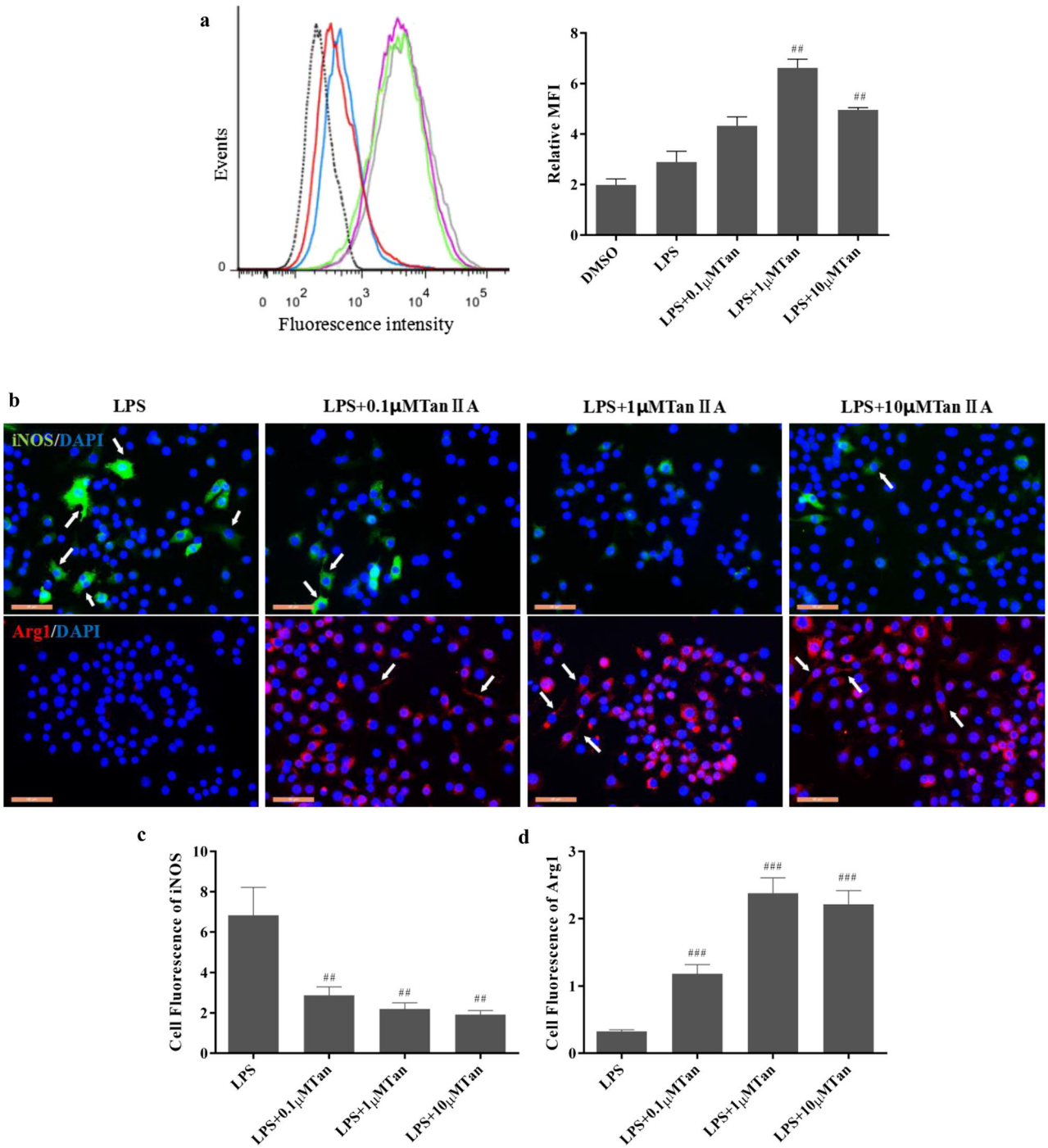

Fig. 4. TanIIA promoted M2 polarization in LPS-stimulated RAW264.7 cells. **a** Representative flow cytometry histograms and averaged relative mean fluorescence intensity (MFI) across three separate experiments of CD206 for 24 h. **b** Fluorescence images of cells immunostained for iNOS (green) and Arg1 (red) and DAPI counterstain (blue) of control, LPS-treated and LPS/TanIIA-treated cells for 24 h (scale bar 50 μm). **c**, **d** Quantification of cell fluorescence for each group. Error bars indicated mean ± SD for three separate experiments. $^{###}p < 0.001$, $^{##}p < 0.01$ compared with the LPS group.

FBGCs) [19] and expressed hyper-fluorescence of iNOS. However, this could be inhibited significantly by TanIIA treatment. We also found that RAW264.7 cells stimulated with TanIIA in the presence of LPS expressed high level of

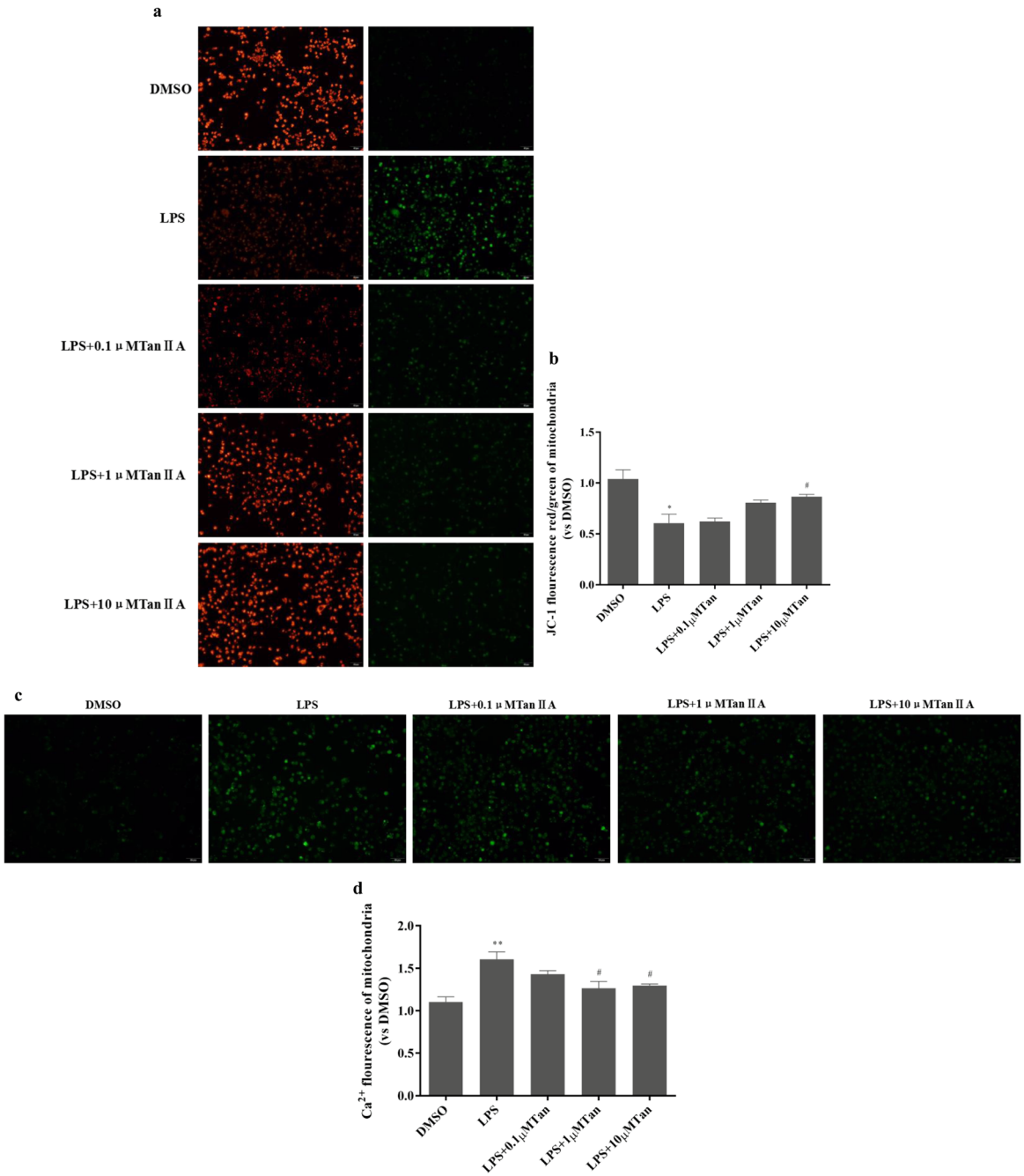

Fig. 5. Polarization of macrophages toward M2 phenotype is associated with changes in mitochondrial function. **a** Representative fluorescence images of cells mitochondrial membrane potential was measured with the JC-1 probe for J-aggregates (red) and monomer (green) of each group (scale bar 50 μm). **b** Mitochondrial membrane potential in mitochondria of each group was measured with the JC-1 probe. **c** Representative fluorescence images of cell calcium overload (Ca^{2+}) was measured with Fluo-4 AM (scale bar 50 μm). **d** Mitochondrial calcium overload (Ca^{2+}) was measured with Fluo-4 AM. **e**–**g** Representative Western blot of Cyc-C, UCP3, and GAPDH from LPS treated or LPS/TanIIA treated for 24 h and quantitative data of average across three separate experiments. Error bars indicated mean ± SD for three separate experiments. $^{***}p < 0.001$, $^{**}p < 0.01$, $^{*}p < 0.05$ compared with the control group; $^{###}p < 0.001$, $^{##}p < 0.01$, $^{#}p < 0.05$ compared with the LPS group.

Arg1, and the cells exhibited more elongated morphologies (Fig. 4b, d) corresponded with the results of 3.1. Together, these data suggested that TanIIA could regulate the polarization and promote M2 phenotype in LPS-stimulated

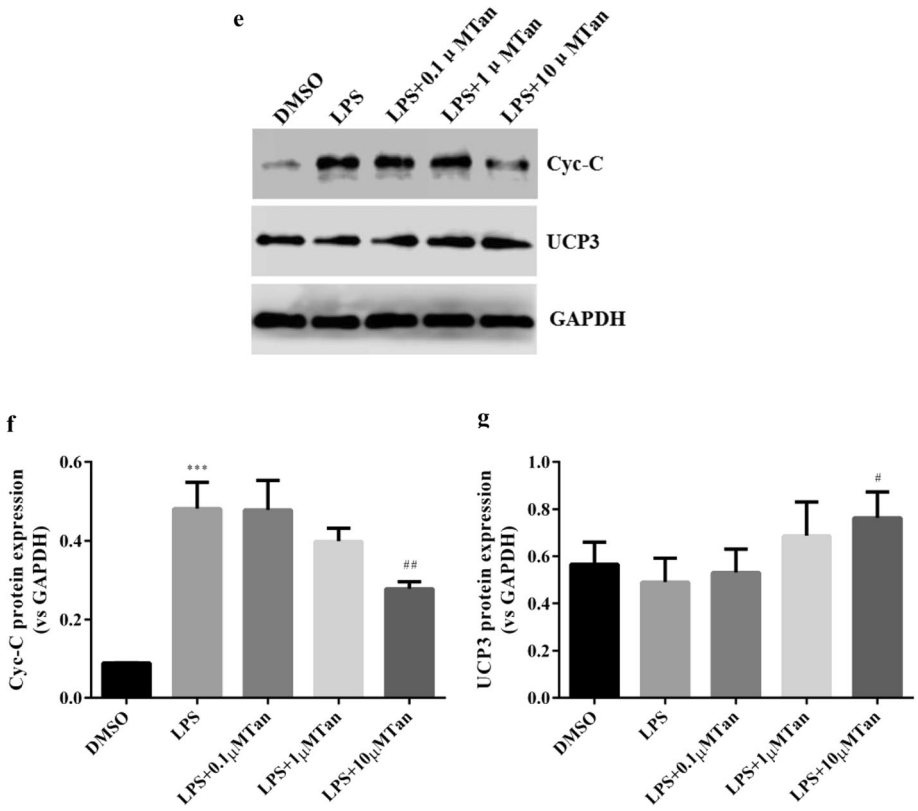

Fig. 5. (continued)

RAW264.7 cells; meanwhile, cell elongation might be associated with M2 macrophage polarization.

TanIIA Promotes M2 Macrophage Polarization in LPS-Stimulated RAW264.7 Cells Along with Changes in Mitochondrial Function

It has been reported that the regulation of cellular metabolism is critical in shaping the macrophage polarization states and immune functions [20]. So we assessed changes of mitochondrial function. As shown in Fig. 5a, b, LPS resulted in significant mitochondrial membrane depolarization in RAW264.7 cells, and TanIIA prevented this from happening. TanIIA also resulted in a decrease of calcium overload compared with that in the LPS group (Fig. 5c, d). The amounts of proteins involved in mitochondrial oxygen metabolism, as assessed by immunoblotting, showed a trend similar to the above result (Fig. 5e–g). These data verified that the regulation of macrophage polarization by TanIIA was achieved by adjusting cell metabolism.

TanIIA Promotes M2 Macrophage Polarization in LPS-Stimulated RAW264.7 Cells Through Changing TLR4-HMGB1/CEBP-β Pathway

Arg1 is primarily regulated by the transcription factors C/EBP-β. Ablation or knockdown of C/EBP-β abrogates Arg1 expression and M2 differentiation [21–23]. In the present study, we also examined expression of several proteins which were involved in pathways of polarization. As shown in Fig. 6a–c, LPS resulted in significantly high level of TLR4 and HMGB1 proteins, and TanIIA could inhibited that. Simultaneously, C/EBP-β protein expression was up-regulated and dependent on the dosage of TanIIA (Fig. 6a, d). The above results demonstrated that TanIIA regulated polarization in LPS-stimulated RAW264.7 cells through affecting key protein concerned in polarized pathways.

DISCUSSION

Previous studies have showed that TanIIA plays a key role in inflammatory response and ventricular remodeling [24–26]. However, the mechanism underlying the effect of

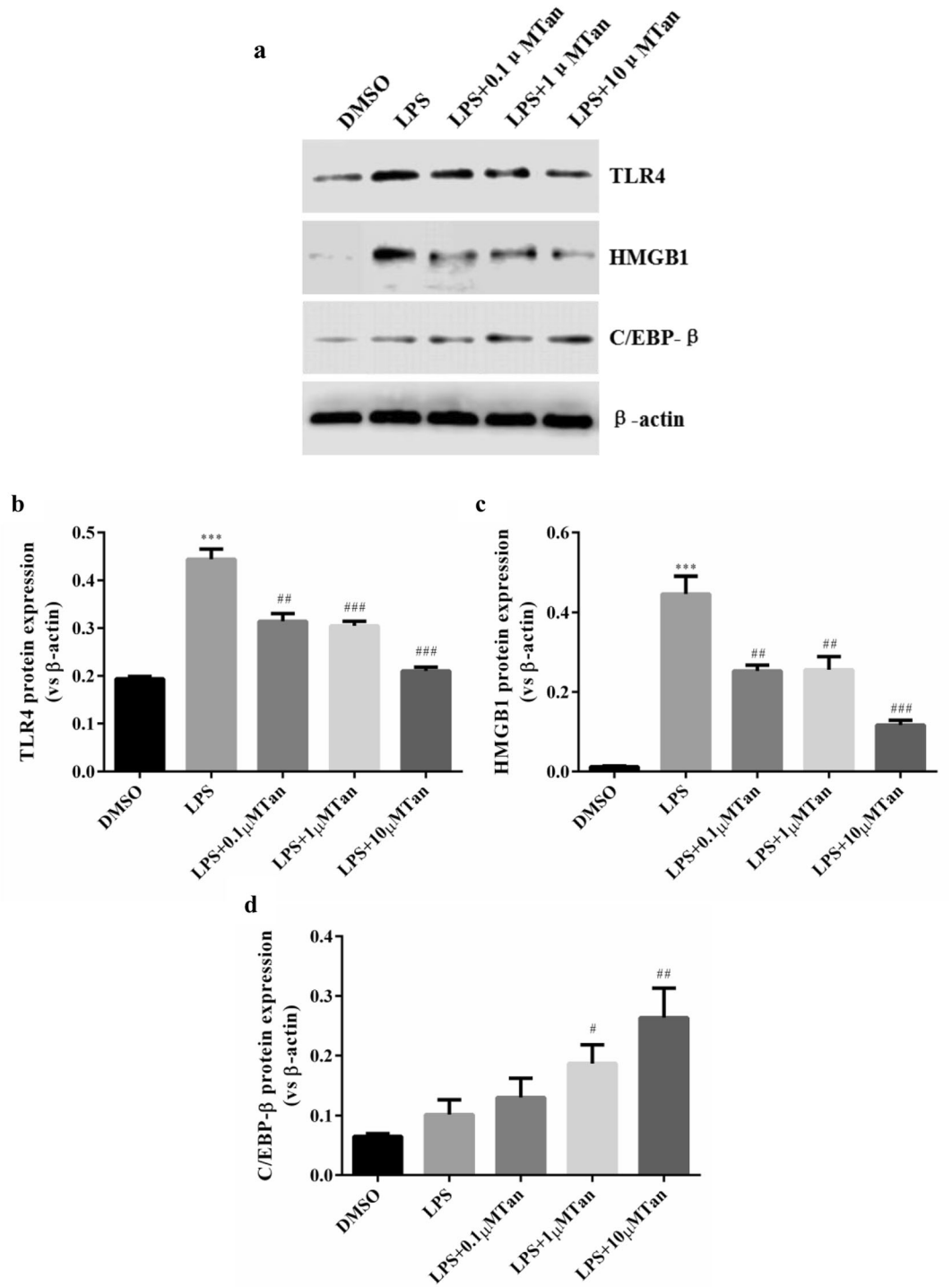

Fig. 6. TanIIA promotes M2 macrophage polarization in LPS-stimulated RAW264.7 cells through changing TLR4-HMGB1/CEBP-β pathway. **a** Representative Western immunoblots for TLR4, HMGB1, and C/EBP-β. **b**–**d** Bar graph showing corresponding quantitative data. Error bars indicated mean ± SD for three separate experiments. ***$p < 0.001$ compared with the control group; $^{###}p < 0.001$, $^{##}p < 0.01$, $^{#}p < 0.05$ compared with the LPS group.

TanIIA was unclear. In the present study, we observed that TanIIA reduced pro-inflammatory response and regulated macrophage polarization in LPS-stimulated RAW264.7 cells, which was supported by several lines of evidence: (1) TanIIA changed the morphology of LPS-stimulated RAW264.7 cells; (2) TanIIA reduced the secretion of TNF-α and increased IL-10; (3) TanIIA inhibited the expressions of iNOS and IL-1β, which were M1 phenotype markers. Meanwhile, TanIIA increased the expressions of Arg1, Fizz1, and CD206, which were M2 phenotype markers; (4) TanIIA promotes M2 macrophage polarization along with changes in mitochondrial function; (5) TanIIA changed the expressions of key protein in TLR4-HMGB1/CEBP-β pathway to promote M2 macrophage polarization.

Cellular morphology and elongation has been shown to influence nuclear organization, chromatin condensation, and histone modification [27], which have an impact on genetic reprograms associated with macrophage phenotype. In our study, TanIIA could indeed make the cells more elongation. Furthermore, an important area of future work is to observe the effect of using TanIIA along with changes in the physical extracellular environment on macrophage polarization and function. Energy metabolism plays a key role in inflammatory reaction and tissue reparation in myocardial infarction, which also has a relationship with macrophage polarization [28]. Mitochondria are catabolic organelles and are the major source of cellular ATP and ROS, which are important in innate immune responses to cellular damage, stress, and infection [29]. Our study showed that TanIIA prevented mitochondrial membrane depolarization and decreased calcium overload. The expressions of UCP3 and Cyc-C also showed that TanIIA could ameliorate mitochondrial function associated with polarization.

Recent observations suggest that metabolic shifts in mitochondrial dynamics may be involved in Toll-like receptor agonist-mediated inflammatory responses and immune cell polarization [30]. TLR4, located on the cell surface, is an important mediator of inflammatory response after myocardial infarction [31]. TLR4 is the only TLR that signals through both MyD88 and TRIF signaling pathways [32]. The present research examined the expression of HMGB1 and C/EBP-β which were mediated through TLR4 pathway. Beyond that, we also detected the expression of miR-155 (Fig. S3). It was reported that silencing miR-155 could reduce myocardial injury and cardiac dysfunction, and promote the polarization of macrophages to M2 phenotype [33]. Meanwhile, miR-155 enhanced the mediation of TLR4-MyD88 signaling pathway by inhibiting the negative regulatory factor SOCS1, promoting the effect of pro-inflammation [34]. Some studies have shown that TRIF-mediated signal pathway can promote the secretion of IL-10, TGF-β, and other cytokines, and collect medullary cells for tissue reparation [35]. However, miR-155 can directly target IKKε to weaken the mediation of TLR4-TRIF signaling pathway [36]. At the same time, miR-155 inhibits the expression of Arg1, a surface marker of M2 macrophages, which is regulated by the expression of C/EBP-β [37]. Thus, miR-155 is in the key position of regulating monocyte/macrophage polarization signal pathway. Remind us that intervening in the expression of miR-155 may be an effective target for suppressing inflammation and promoting reparation. Our data suggested that TanIIA could downregulate the expression of miR-155. Nevertheless, the mechanisms need to be clarified in our later study.

Collectively, these findings provide new insights into the mechanism of TanIIA and its therapeutic potential in the treatment of myocardial infarction.

FUNDING INFORMATION

This study was supported by the Tianjin Outstanding Youth Science Foundation (No. 17JCJQJC46200), the National Natural Science Foundation of China (No. 81774050), the National Key Basic Research Program of China (No. 2012CB518404), the Foundation of First Teaching Hospital of Tianjin University of Traditional Chinese Medicine (No. 201703), and the Tianjin Science and Technology Program: Tianjin TCM Clinical Medicine Research Center (No. 15ZXLCSY00020).

COMPLIANCE WITH ETHICAL STANDARDS

Conflict of Interest. The authors declare that there are no conflicts of interest.

REFERENCES

1. Mann, Douglas L. 2015. Innate immunity and the failing heart the cytokine hypothesis revisited. *Circulation Research* 116: 1254–1268.
2. Mantel, Ä., M. Holmqvist, D.C. Andersson, L.H. Lund, and J. Askling. 2017. Association between rheumatoid arthritis and risk of ischemic and nonischemic heart failure. *Journal of the American College of Cardiology* 69: 1275–1285.
3. Ridker, P.M., J.G. MacFadyen, B.M. Everett, et al. 2017. Relationship of C-reactive protein reduction to cardiovascular event reduction following treatment with canakinumab: a secondary analysis from the CANTOS randomized controlled trial. In *Lancet*.
4. Ridker, P.M., J.G. MacFadyen, T. Thuren, et al. 2017. Effect of interleukin-1β inhibition with canakinumab on incident lung cancer in patients with atherosclerosis: exploratory results from a

randomized, double-blind, placebo-controlled trial. In *Lancet*, vol. 390, 1833–1842.
5. Ridker, P.M., B.M. Everett, T. Thuren, et al. 2017. Antiinflammatory therapy with canakinumab for atherosclerotic disease. *The New England Journal of Medicine*: 377.
6. Borthwick, L.A., L. Barron, K.M. Hart, K.M. Vannella, R.W. Thompson, S. Oland, A. Cheever, J. Sciurba, T.R. Ramalingam, A.J. Fisher, and T.A. Wynn. 2016. Macrophages are critical to the maintenance of IL-13-dependent lung inflammation and fibrosis. *Mucosal Immunology* 9: 38–55.
7. Ginhoux, F., J.L. Schultze, P.J. Murray, et al. 2015. New insights into the multidimensional concept of macrophage ontogeny, activation and function. *Nature Immunology* 17: 34–40.
8. Murray, Peter J. 2017. Macrophage polarization. *Annual Review of Physiology* 79: 2.1–2.26.
9. McWhorter FY, Wang T, Nguyen P, et al. 2013. Modulation of macrophage phenotype by cell shape. Proceedings of the National Academy of Sciences of the United States of America 110: 17253–17258.
10. Jha, A.K., S.C. Huang, A. Sergushichev, et al. 2015. Network integration of parallel metabolic and transcriptional data reveals metabolic modules that regulate macrophage polarization. *Immunity* 42: 419–430.
11. Ouimet, M., H.N. Ediriweera, U.M. Gundra, F.J. Sheedy, B. Ramkhelawon, S.B. Hutchison, K. Rinehold, C. van Solingen, M.D. Fullerton, K. Cecchini, K.J. Rayner, G.R. Steinberg, P.D. Zamore, E.A. Fisher, P'. Loke, and K.J. Moore. 2015. MicroRNA-33-dependent regulation of macrophage metabolism directs immune cell polarization in atherosclerosis. *The Journal of Clinical Investigation* 125: 4334–4348.
12. Van den Bossche, J., J. Baardman, N.A. Otto, et al. 2016. Mitochondrial dysfunction prevents repolarization of inflammatory macrophages. *Cell Reports* 17: 684–696.
13. Son, M., A. Porat, M. He, J. Suurmond, F. Santiago-Schwarz, U. Andersson, T.R. Coleman, B.T. Volpe, K.J. Tracey, Y. al-Abed, and B. Diamond. 2016. C1q and HMGB1 reciprocally regulate human macrophage polarization. *Blood* 128: 2218–2228.
14. Katare, P.B., P.K. Bagul, A.K. Dinda, and S.K. Banerjee. 2017. Toll-like receptor 4 inhibition improves oxidative stress and mitochondrial health in isoproterenol-induced cardiac hypertrophy in rats. *Frontiers in Immunology* 8.
15. Bala, S., T. Csak, B. Saha, et al. 2016. The pro-inflammatory effects of miR-155 promote liver fibrosis and alcohol-induced steatohepatitis. *Journal of Hepatology* 64: 1–32.
16. Wang, D., Y. Liu, G. Zhong, Y. Wang, T. Zhang, Z. Zhao, X. Yan, and Q. Liu. 2017. Compatibility of Tanshinone IIA and Astragaloside IV in attenuating hypoxia-induced cardiomyocytes injury. *Journal of Ethnopharmacology* 204: 67–76.
17. Lobo-Silva, D., G.M. Carriche, A.G. Castro, S. Roque, and M. Saraiva. 2017. Interferon-β regulates the production of IL-10 by toll-like receptor-activated microglia. *Glia* 65: 1439–1451.
18. Hagert, C., O. Sareila, T. Kelkka, S. Jalkanen, and R. Holmdahl. 2018. The macrophage mannose receptor regulate Mannan-induced psoriasis, psoriatic arthritis, and rheumatoid arthritis-like disease models. *Frontiers in Immunology* 9.
19. Klopfleisch, R. 2016. Macrophage reaction against biomaterials in the mouse model-phenotypes, functions and markers. *Acta Biomaterialia* 43: 3–13.
20. Teng, O., C.K.E. Ang, and X.L. Guan. 2017. Macrophage-bacteria interactions-a lipid-centric relationship. *Frontiers in Immunology* 8.
21. Arranz A, Doxaki C, Vergadi E, Martinez de la Torre Y, Vaporidi K, Lagoudaki ED, Ieronymaki E, Androulidaki A, Venihaki M, Margioris AN, Stathopoulos EN, Tsichlis PN, Tsatsanis C 2012. Akt1 and Akt2 protein kinases differentially contribute to macrophage polarization. Proceedings of the National Academy of Sciences of the United States of America 109: 9517–9522.
22. Sahu, S.K., M. Kumar, S. Chakraborty, S.K. Banerjee, R. Kumar, P. Gupta, K. Jana, U.D. Gupta, Z. Ghosh, M. Kundu, and J. Basu. 2017. MicroRNA 26a (miR-26a)/KLF4 and CREB-C/EBP-β regulate innate immune signaling, the polarization of macrophages and the trafficking of Mycobacterium tuberculosis to lysosomes during infection. *PLoS Pathogens* 13: e1006410.
23. Na, Y.R., D. Jung, B.R. Yoon, W.W. Lee, and S.H. Seok. 2015. Endogenous prostaglandin E2 potentiates anti-inflammatory phenotype of macrophage through the CREB-C/EBP-β cascade. *European Journal of Immunology* 45: 2661–2671.
24. Liu, X., and J. Meng. 2018. Tanshinone IIA ameliorates lipopolysaccharide-induced inflammatory response in bronchial epithelium cell line BEAS-2B by down-regulating miR-27a. *Biomedicine & Pharmacotherapy* 104: 158–164.
25. Luan, L., and Z. Liang. 2018. Tanshinone IIA protects murine chondrogenic ATDC5 cells from lipopolysaccharide-induced inflammatory injury by down-regulating microRNA-203a. *Biomedicine & Pharmacotherapy*: 628–636.
26. Wu, D.M., Y.J. Wang, X.R. Han, et al. 2018. Tanshinone IIA prevents left ventricular remodelling via the TLR4/MyD88/NF-κB signalling pathway in rats with myocardial infarction. *Journal of Cellular and Molecular Medicine*: 1–15.
27. Versaevel, M., T. Grevesse, and S. Gabriele. 2012. Spatial coordination between cell and nuclear shape within micropatterned endothelial cells. *Nature Communications* 3.
28. Wang, L., and Q. Ma. 2018. Clinical benefits and pharmacology of Scutellarin: a comprehensive review. *Pharmacology & Therapeutics*.
29. Sena, L.A., S. Li, A. Jairaman, et al. 2013. Mitochondria are required for antigen-specific T cell activation through reactive oxygen species signaling. *Immunity* 38: 1–12.
30. Gao, Z., Y. Li, F. Wang, T. Huang, K. Fan, Y. Zhang, J. Zhong, Q. Cao, T. Chao, J. Jia, S. Yang, L. Zhang, Y. Xiao, J.Y. Zhou, X.H. Feng, and J. Jin. 2017. Mitochondrial dynamics controls anti-tumour innate immunity by regulating CHIP-IRF1 axis stability. *Nature Communications* 8: 1805.
31. Katare, P.B., P.K. Bagul, A.K. Dinda, and S.K. Banerjee. 2017. Toll-like receptor 4 inhibition improves oxidative stress and mitochondrial health in isoproterenol-induced cardiac hypertrophy in rats. In *Front Immunol*, vol. 8.
32. Parkunan, S.M., C.B. Randall, P.S. Coburn, R.A. Astley, R.L. Staats, and M.C. Callegan. 2015. Unexpected roles for toll-like receptor 4 and TRIF in intraocular infection with gram-positive bacteria. *Infection and Immunity* 83: 3926–3936.
33. Zhang, Y., M. Zhang, X. Li, et al. 2016. Silencing microRNA-155 attenuates cardiac injury and dysfunction in viral myocarditis via promotion of M2 phenotype polarization of macrophages. *Scientific Reports*.
34. Smith, T.D., M.J. Tse, E.L. Read, et al. 2016. Regulation of macrophage polarization and plasticity by complex activation signals. *Integrative Biology (Camb)* 8: 1–34.
35. Meng, S., P. Chanda, R.A. Thandavarayan, et al. 2017. Transflammation: innate immune signaling in nuclear reprogramming. *Advanced Drug Delivery Reviews*.
36. Yee, D., K.M. Shah, M.C. Coles, et al. 2017. MicroRNA-155 induction via TNF-α and IFN-γ suppresses expression of programmed death ligand-1 (PD-L1) in human primary cells. *The Journal of Biological Chemistry* 292: 1–9.
37. Bala, S., T. Csak, B. Saha, et al. 2016. The pro-inflammatory effects of miR-155 promote liver fibrosis and alcohol-induced steatohepatitis. *Journal of Hepatology* 64: 1–33.